Nuclear Explosive Pulverization of Basalt

rsk

July 2025

1 Introduction

The pulverization and dispersal dynamics of basalt seafloor are absolutely central to the feasibility of nuclear-explosive based carbon sequestration. of the literature on rock blasting starts with a calculation of the median particle size using the semi-empirical formula of Kutznetsov (1973), or variations developed by Cunningham and others; which is then used to fit a Rosin-Rammler distribution of particle sizes. This is known as the Kuz-Ram model. Rosin-Rammler, like all the particle-size distributions used in the blasting industry, are 'mass passing,' meaning they are cumulative distribution functions describing the fraction of the total mass that can pass through a sieve of a given size. Rosin-Rammler does very well for describing particles in the 20–80 percentiles under normal blasting conditions, but it significantly underestimates the production of fines while also permitting fragment sizes to grow unbounded.[1]

To fix this problem, a more advanced 3-parameter distribution, known as the Swebrec distribution, was later developed. Sieving campaigns show that the Swebrec distribution does extremely well in general, often fitting experimental data with $R^2 > 0.97$. However, using Swebrec to estimate the fine dusts produced by a nuclear explosion still presents two challenges. First, the distribution must be calibrated to the specific charge. At high specific charges (greater than $\sim$ 2 kg-TNT m^{-3}), there is an inflection in the median particle size per unit specific charge, while the distribution still holds, the higher explosive do not shift the median as dramatically.[2] A "double fan" model was proposed in 2021

[1] For the relevant history here, see: Finn Ouchterlony, José A. Sanchidrián, and Peter Moser, "Percentile Fragment Size Predictions for Blasted Rock and the Fragmentation–Energy Fan," *Rock Mechanics and Rock Engineering* 50, no. 4 (April 2017): 751–79, `https://doi.org/10.1007/s00603-016-1094-x`.

[2] A further consideration is the considerably sharper impulse (higher rise time of the pressure wave) from a nuclear blast relative to a chemical explosion. This may also change the fracture dynamics. Past studies have found that as the impulse increases, the pulverization process dominates over the formation of long cracks. This suggests that estimates drawn from chemical blasts may underestimate the production of particles. See: Xu, Xuan, et al. "Insight into Rock Fragmentation and Damage Affected by Temporal Characteristics of Blast Loading," *Rock Mechanics and Rock Engineering* 58, no. 5, 2025, 5405–27. `https://doi.org/10.1007/s00603-025-04389-9`.

by Ouchterlony et al. in order to rectify this.[3]

The second challenge is that the shape of the Swebrec distribution begins to deviate from empirical data in the far ends of the tails. Indeed, once below the grain size, the underlying physics of fragmentation changes, so it is not *a priori* evident that the distribution should hold in this super-fine regime, which is the regime of greatest interest to the carbon sequestration problem.

To improve the semi-empirical estimation of super-fine dusts, a five-parameter extended Swebrec was developed, which has been shown to reproduce sieving data down to 75–100 μm, well below the grain size.[4] Fitting this function requires data in the super-fine regime, however, which is not usually obtained in normal sieving campaigns. Additionally, we are particularly interested in ultra-fine particles ($< 10\mu$m), an extrema below where even the extended Swebrec has been validated.

An alternative approach to estimating production in the ultra-fine regime would be to use a physics-based theoretical model of brittle fragmentation, such as the branch-merge fractal model that gives rise to a scale-invariant power law in the fine domain for particles below the grain size.[5] This approach has been validated at very high energy densities, even as high as 60 kgTNT m^{-3}, which as we will show, includes the energy densities of very large nuclear blasts. The model is widely used in rock mechanics, modeling asteroid collisions, etc.[6]

In this paper, we shall splice together the 3-parameter Swebrec and the fractal model at the transitions size x_t, giving this piecewise distribution for the mass-passing cumulative distribution function:

$$F(x) = \begin{cases} \left(\dfrac{x}{x'_{\max}}\right)^{3-D}, & x < x_t, \\ \left[1 + \left(\dfrac{\ln(x_{\max}/x)}{\ln(x_{\max}/x_{50})}\right)^{b}\right]^{-1}, & x \geq x_t. \end{cases} \tag{1}$$

Here $F(x)$ is the mass fraction of the total pulverized rock particles that able to pass through a sieve with mesh size x, which we will take as being approximately the diameter of the particle. The Swebrec function is that which describes the distribution for most of the particles with sizes above the transition size. The parameter $x_{\max}$ is a notional largest fragment size generated by the blast, x_{50} is the size at which 50% of the mass lies above and 50% lies below , which is a function of the specific charge, and b is the curvature or 'undulation' exponent.

[3] Ouchterlony, Finn, José A. Sanchidrián, and Ömürden Genç. 2021. "Advances on the Fragmentation-Energy Fan Concept and the Swebrec Function in Modeling Drop Weight Testing," *Minerals* 11, no. 11: 1262. https://doi.org/10.3390/min11111262.

[4] José A. Sanchidrián et al., "Performance of Some Distributions to Describe Rock Fragmentation Data," *International Journal of Rock Mechanics and Mining Sciences* 53 (July 2012): 18–31. https://doi.org/10.1016/j.ijrmms.2012.04.001.

[5] J.A. Åström et al., "Universal Dynamic Fragmentation in D Dimensions," *Physical Review Letters* 92, no. 24 (June 18, 2004), https://doi.org/10.1103/physrevlett.92.245506.

[6] Charles G. Sammis and Ronald L. Biegel, "Fractals, Fault-Gouge, and Friction," *Pure and Applied Geophysics* 131, no. 1–2 (1989): 255–271, https://doi.org/10.1007/BF00874490; Donald L. Turcotte, "Fractals and Fragmentation," *Journal of Geophysical Research: Solid Earth* 91, no. B2 (1986): 1921–1926, https://doi.org/10.1029/JB091iB02p01921.

All of the required parameters are determined by fits to sieving campaigns from rock blasts on the specific kind of rock under study (n.b., strong changes in energy regime require re-estimation of b whereas similar energy regimes tend to share a b).

Below the transition size x_t, we shall switch to the theoretical model. We shall set the transition size to be equal to that typical grain size of basalt ($\approx$ 0.3 mm). Since the Swebrec region ($x > x_t$) is supported by data-rich empirical observations, we shall fit its parameters from these observations. The parameters for the theoretical model will then be selected to form a continuous (but not necessarily smooth) join to the Swebrec distribution. The parameter D, is the fractal dimension of the fragment population. Studies find that typically $2 < D < 3$, where higher fragmentation energy or strain rates leading to higher fractal dimensions. For an energy density equal to the specific charge of our nuclear blast (8.4×10^4 J/kg in basalt, computed below, data from Buhl et al. (2014) suggest a trend that places $D \approx 3$ in the nuclear-blast regime.[7] If we adopt this prediction, the joining of the two models will occur by tuning $x'_{\max}$, which is the notional upper-bound particle size in the theoretical model.

2 Specific Charge

To begin, we first need to estimate the specific charge for a nuclear blast (specific energy per unit volume, with energy written in terms of kilograms of TNT-equivalent) for the blast. The pulverized volume depends significantly on the depth of burial, as illustrated in figure 1.

Glasstone and Dolan[8] give scaling relationships for craters produced by nuclear explosions. In this study, we assume that fine dust will settle slowly according to the Stoke's settling velocity. Since these are the fines that are needed to sequestration, we consider the case where the blast lifts these into the water and the settle along the top surface, where ocean currents react. In this case, we want to maximize the ejecta. The depth that maximizes the ejecta volume in hard wet rock is

$$d^* = 40 \text{ m} \cdot \left(\frac{W}{1 \text{ kt}}\right)^{0.3},$$

where W is the explosive yield (nominally in kilotons of TNT equivalent). As an example, the 1.2 MT B83 nuclear weapon from the U.S. arsenal would have an optimal depth of burial of about 340 meters.

Assuming optimal burial is achieved, the resulting crater has both an apparent depth (that remaining above the fallback rubble) and a true depth (the interface of the evacuated area, now partially refilled with fallback rubble, and the surface of the original rock mass) as shown in figure 2.

[7] Xu Yongfu, "The fractal evolution of particle fragmentation under different fracture energy," *Powder Technology* 322:1 (Jan 2018), 337–345. `https://doi.org/10.1016/j.powtec.2017.10.011`

[8] Samuel Glasstone and Philip J. Dolan, *The Effects of Nuclear Weapons,* Third ed. (U.S. Atomic Energy Commission, 1977).

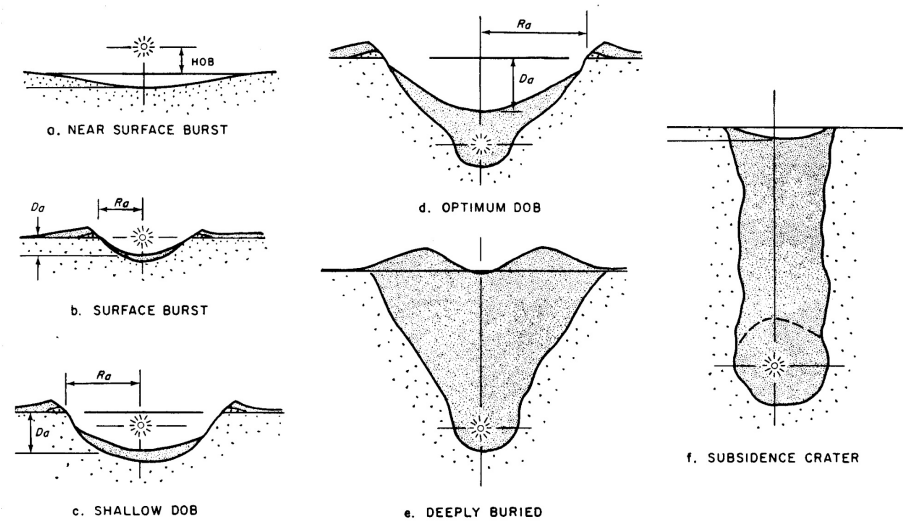

Figure 1: Types of cratering effects formed by explosions at different depths.

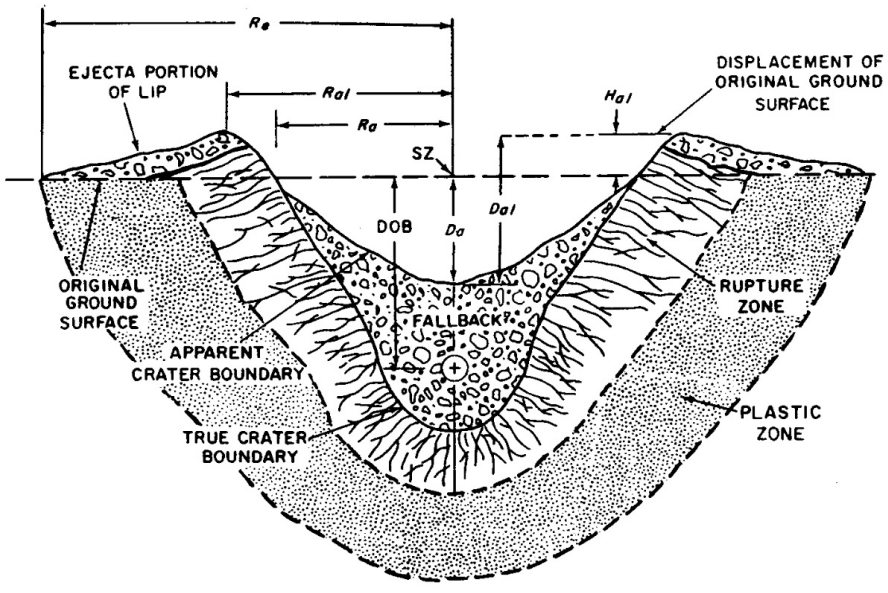

Figure 2: Anatomy of an optimal crater.

Since we need to find the charge density of the pulverized rock volume, we first need to estimate the total volume of the true crater. Glasstone and Dolan describe the evacuated zones as approximately parabolic, and a relationship is given for the apparent depth (D_a in Figure 2), but not the true depth.[9]

To estimate the true depth, let us assume that the optimal depth of burial is the focus of a parabola tracing out the true crater boundary. Under this assumption, we can estimate the true depth (the vertical distance from the vertex of the parabola to the original seafloor) using just R_a, and the depth of burst d^*, as:

$$D_{\text{true}} = \frac{\sqrt{(d^*)^2 + R_a^2} - d^*}{2},$$

where the apparent radius R_a is given by Glasstone and Dolan as

$$R_a = 46 \text{ m} \cdot \left(\frac{W}{1 \text{ kt}} \right)^{0.3}.$$

The (true) crater volume, estimated as a paraboloid, is

$$V = \frac{\pi}{2} D_{\text{true}} R_a^2,$$

and the specific charge is

$$q = \frac{W}{V} \approx 29 W[\text{kt}]^{0.1} [\text{kgTNT/m}^3].$$

For our B83 example, this computes to a specific charge of 59 kgTNT/m^3 = 2.5$\times$ 10^8 J/m^3 = 8.4$\times$10^4 J/kg-rock, (assuming basalt's density is 2.95 g/cm^3). Note that this is about 100 times the specific charge typically used in conventional blasting, which places this into a high-energy regime and affects our ability to predict the median particle size using traditional blast data.

3 Estimation of the Swebrec fit parameters

To calibrate the Swebrec function, we need to predict the particle sizes at which different percentiles in the mass passing fraction occur. These can be obtained for an arbitrary specific charge using the fragmentation-energy fan method. Specifically, this approach is based on the observation that when the logarithm of sieve size is plotted against the logarithm of the specific charge, all the data for a given mass-passing percentile (regardless of the specific charge) will lie in a straight line in log-log space. The different percentiles form a set of lines, each with a different slope converging at a single focal point that depends on the type

[9] We are interested in very fine particles, which have very slow Stokes settling velocities, and we will assume that rock fragments from the entire volume of the true crater participates in the production of such particles.

of rock being blasted, thus forming a 'fan' shape.[10] However, once the specific charge exceeds roughly 2 kgTNT m^{-3}—the exact threshold depends on the material—the blast enters the high-energy regime and the straight lines exhibit a kink and turn to a more shallow slope.[11] This occurs well above the specific charges for normal blasting, but well below the specific charge of a nuclear blast. This regime, is found mainly in mechanical rock crushing. To cope with this regime, the double fan theory was developed that joins the two slopes for each percentile class at the inflection points.

From the fragmentation-energy-fan theory[12], we have

$$b = \frac{\ln\left(\frac{1-P}{P}\right)}{\ln(\alpha_p/\alpha_{50})}$$

where P is any percentile class other than $P = 50$.

3.1 Basalt

For "very fresh basalt," sieving data from Faramarzi are published as Figure A6.1 in Ouchterlony et al.[13], which is reproduced here as Fig. 3.

Ouchterlony et al. (2021) report in the text that for basalt, the Swebrec undulation parameter of our Eq. 1 was found to be $b = 2.19 \pm 0.27$. They also report that the log-space slope of the 50^{th}-percentile line in the high-energy fan is $\alpha_{50}^{\text{H}} = 0.8817$. Other data in Fig. 3 have been non-dimensionalized in terms of particle sizes and scaled in terms of blast energy.

An expression for the median (50^{th}-percentile) fan line in the high-energy regime (H) is given by

$$x'^{\text{H}}_{50} = CE'^{-\alpha^{\text{H}}_{50}}.$$

Inserting α^{H}_{50}, and solving for C using the intersect point $(E'_0, x'_0) = (0.0719, 1.8031)$, we have:

$$x'^{\text{H}}_{50} = 0.177E'^{-0.8817}. \tag{2}$$

The same procedure for the 20^{th}-percentile fan line in the high-energy regime will give

$$x'^{\text{H}}_{20} = 0.05225E'^{-1.3452}. \tag{3}$$

[10] Finn Ouchterlony, José A. Sanchidrián, and Peter Moser, "Percentile Fragment Size Predictions for Blasted Rock and the Fragmentation–Energy Fan," *Rock Mechanics and Rock Engineering* 50, no. 4 (April 2017): 751–79, https://doi.org/10.1007/s00603-016-1094-x.

[11] Ouchterlony, Finn, José A. Sanchidrián, and Ömürden Genç. 2021. "Advances on the Fragmentation-Energy Fan Concept and the Swebrec Function in Modeling Drop Weight Testing" *Minerals* 11, no. 11: 1262. https://doi.org/10.3390/min11111262

[12] Finn Ouchterlony, José A. Sanchidrián, and Peter Moser, "Percentile Fragment Size Predictions for Blasted Rock and the Fragmentation–Energy Fan," *Rock Mechanics and Rock Engineering* 50, no. 4 (April 2017): 751–79, https://doi.org/10.1007/s00603-016-1094-x.

[13] Ouchterlony, Finn, José A. Sanchidrián, and Ömürden Genç. 2021. "Advances on the Fragmentation-Energy Fan Concept and the Swebrec Function in Modeling Drop Weight Testing" Minerals 11, no. 11: 1262. https://doi.org/10.3390/min11111262

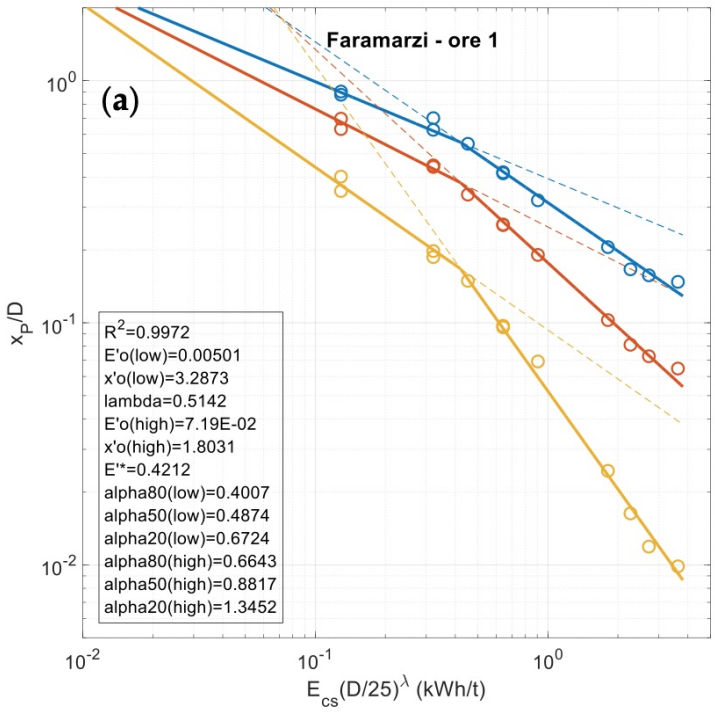

Figure 3: The double fragmentation-energy fan for Basalt samples collected by Faramarzi reported as Figure A6 in Ouchterlony et al. (2021) . Yellow is the 20^{th} percentile, red is the 50^{th}, and blue is the 80^{th}. Note that here D is the original particle size before crushing, equivalent to $x_{\max}$, and the axes have been non-dimensionalized.

We now make the change of variables to rescale the energy and redimensionalize the particle size:

$$E' \Rightarrow E_{\text{cs}}(D/D_0)^{\lambda} = E_{\text{cs}}(x_{\max}/25\text{ mm})^{0.5142}$$

$$x_p'^{\text{H}} \Rightarrow x_p/D$$

giving expressions in D. Noting also that, per Ouchterlony et al., $D \equiv x_{\max}$, we have:

$$(x_{\max}/x_{50}^{\text{H}}) = \left[0.177(E_{\text{cs}}(x_{\max}/25\text{ mm})^{0.5142})^{-0.8817}\right]^{-1}$$

$$(x_{\max}/x_{20}^{\text{H}}) = \left[0.05225(E_{\text{cs}}(x_{\max}/25\text{ mm})^{0.5142})^{-1.3452}\right]^{-1},$$

which we can related to each other through the Swebrec function showing in Eq. 1, reproduced here:

$$F(x) = \left[1 + \left(\frac{\ln(x_{\max}/x)}{\ln(x_{\max}/x_{50})}\right)^{b}\right]^{-1}$$

Which for the 20$^{\text{th}}$-percentile gives us:

$$0.2 = \left[1 + \left(\frac{\ln(x_{\max}/x_{20})}{\ln(x_{\max}/x_{50})}\right)^{b}\right]^{-1}$$

$$0.2 = \frac{1}{1 + \left(\dfrac{\ln\left[19.1388\left(E_{\text{cs}}\left(\frac{x_{\max}}{25\ \text{mm}}\right)^{0.5142}\right)^{1.3452}\right]}{\ln\left[5.64972\left(E_{\text{cs}}\left(\frac{x_{\max}}{25\ \text{mm}}\right)^{0.5142}\right)^{0.8817}\right]}\right)^{2.19}}$$

Solving now for $x_{\max}$, we have

$$x_{\max} = (25\ \text{mm}) \cdot 0.14833 E_{\text{cs}}^{-1.94477}$$

Here E_{cs} is the specific communition energy in units kWh/tonne$_{\text{rock}}$, which is the energy version of the specific charge calculated in section 2. We computed that for our 1 MT explosive we have 8.4×10^4 J/kg-rock = 23 kWh/tonne, which is the appropriate units for these relations. This gives $x_{\max} = 8.3$ µm, which is not very credible.

In fact, by comparison to the inflection point, we find our energy is actually in the low-energy regime, but re-computation from the low-energy fan still doesn't produce a physically realistic value.

The log-space slope of the 50$^{\text{th}}$-percentile line in the *low-energy* fan is $\alpha_{50}^{\ell} = 0.4874$. Using the intersect point $(E_0'^{\ell}, x_0'^{\ell}) = (0.00501, 3.2873)$, we have:

$$\left(\frac{x_{\max}}{x_{50}^{\ell}}\right) = \left[0.24874\left(E_{\text{cs}}\left(\frac{x_{\max}}{25\ \text{mm}}\right)^{0.5142}\right)^{-0.4874}\right]^{-1},$$

$$\left(\frac{x_{\max}}{x_{20}^{\ell}}\right) = \left[0.09337\left(E_{\text{cs}}\left(\frac{x_{\max}}{25\ \text{mm}}\right)^{0.5142}\right)^{-0.6724}\right]^{-1}.$$

Relating these through the Swebrec function

$$0.2 = \frac{1}{1 + \left(\dfrac{\ln\left[\underbrace{10.7100}_{1/0.09337}\left(E_{\text{cs}}\left(\frac{x_{\max}}{25\ \text{mm}}\right)^{0.5142}\right)^{0.6724}\right]}{\ln\left[\underbrace{4.02031}_{1/0.24874}\left(E_{\text{cs}}\left(\frac{x_{\max}}{25\ \text{mm}}\right)^{0.5142}\right)^{0.4874}\right]}\right)^{2.19}}.$$

Solving now for $x_{\max}$, we obtain

$$x_{\max} = (25\ \text{mm}) \cdot \underbrace{0.13897}_{\exp\left(\frac{T}{\lambda}\right)} E_{\text{cs}}^{-1/\lambda} = (25\ \text{mm}) \cdot 0.13897\, E_{\text{cs}}^{-1.94477},$$

where $T = \dfrac{R\ln(4.02031) - \ln(10.7100)}{\alpha_{20}^{\ell} - R\,\alpha_{50}^{\ell}}$ and $R = \left(1/0.2 - 1\right)^{1/b} = 4^{1/2.19}$. For $E_{\text{cs}} = 23$ kWh/tonne in the low-energy regime, we find $x_{\max} = 7.8$ µm, which is still nonphysical.

There are blasting (rather than dropweight testing) data for other ores such as hornfels and reddish gray granite from Vändle aggregate quarry. The extent to which these are similar to basalt is unclear. Some have similar unilateral compressive strength (UCS) and brittleness index—which are the two best predictors of fragmentation dynamics in the literature.[14] However, these data are well below the nuclear-blasting regime.

[14]Note that the brittleness index incorporates UCS, as it is defined as the static (Young's) deformation modulus divided by UCS. Fragmentation is driven primarily by dynamic tensile failure, and UCS is a practical surrogate for both dynamic tensile strength and fracture toughness. Young's modulus affects wave velocity and energy storage, so it matters, but only after strength and explosive energy have been accounted for. Packaging the two into the brittleness index discards the temporal ordering and so may have less predictive power relative to UCS alone. Nevertheless, hornfels was selected for its similarity in both regards.

Variables Names

Symbol	Meaning	Units	Definition / Notes
x_p	Percentile fragment size (at $p\%$)	length	Generic percentile; typical $p \in \{20, 50, 80\}$.
x_{20}, x_{50}, x_{80}	Specific percentiles	length	Instances of x_p.
x	Sieve size variable in CDF $P(x)$	length	Independent variable in Swebrec.
$x_{\max}$	Maximum fragment size parameter	length	Upper size limit in Swebrec model.
$x'_{\max}$	Maximum fragment size parameter	length	Upper size limit in theoretical fractal model
D	Progeny particle size for drop-weight tested (DWT) particles	length	Upper size limit in DWT version of Swebrec; assumed equivlant to $x_{\max}$
D_0	Reference size for scaling	length	In the Ouchterlony paper, $D_0 = 25$ mm.
x'_p	Dimensionless size	dimensionless	$x'_p = x_p/D$.
E_{cs}	Specific comminution energy	kWh/t	Dimensional abscissa (energy per tonne).
E'_{cs}	D-scaled energy (used in fits)	kWh/t	$E'_{\mathrm{cs}} = E_{\mathrm{cs}}(D/D_0)^{\lambda}$.
E^*	Fan kink (scaled-energy domain)	kWh/t	Transition energy in the E'_{cs} domain.
$E^*_{\mathrm{cs}}(D)$	Fan kink (dimensional)	kWh/t	$E^*_{\mathrm{cs}}(D) = E^*/(D/D_0)^{\lambda}$.
x_0^r	Fan focal size (scaled domain)	dimensionless	$r \in \{p, s\}$: primary/secondary branch.
E_0^r	Fan focal energy (scaled domain)	kWh/t	Intercept energy in E'_{cs} domain.
$\widetilde{x}_0^r(D)$	Fan focal size (dimensional)	length	$\widetilde{x}_0^r(D) = D\, x_0^r$.
$\widetilde{E}_0^r(D)$	Fan focal energy (dimensional)	kWh/t	$\widetilde{E}_0^r(D) = E_0^r/(D/D_0)^{\lambda}$.
α_p^r	Fan slope (percentile p)	dimensionless	Exponent; e.g., $\alpha_{20}^{p/s}, \alpha_{50}^{p/s}, \alpha_{80}^{p/s}$.
λ	Size–energy scaling exponent	dimensionless	From Fig. A6 axis normalization.
q_{t}	Specific charge (per tonne)	kg/t	Powder factor by mass per rock tonne.
q	Specific charge (per volume)	kg/m^3	Per-volume convention.
ρ	Rock bulk density	t/m^3	For conversion $q_{\mathrm{t}} = q/\rho$.
ζ	Energy–charge factor	kWh/kg	$E_{\mathrm{cs}} = \zeta\, q_{\mathrm{t}}$.
η	Effective energy transfer	dimensionless	Fraction of explosive energy imparted.
H_e	Explosive detonation energy	MJ/kg	Typical 3–5 MJ/kg (ANFO $\sim$ 3.8).
$Q_0^r(D)$	Fan focal charge (dimensional)	kg/t	$Q_0^r(D) = \widetilde{E}_0^r(D)/\zeta$.
$q^*(D)$	Charge at kink (dimensional)	kg/t	$q^*(D) = E^*_{\mathrm{cs}}(D)/\zeta$.
$P(x)$	Cumulative passing (Swebrec)	dimensionless	$P(x) = \left[1 + (\ln(x_{\max}/x)/\ln(x_{\max}/x_{50}))^b\right]^{-1}$.
b	Swebrec shape exponent (“undulation parameter”)	dimensionless	Derived from fan slopes (material parameter).

Indicies

Index	Meaning
p	Percentile index (typically $20, 50, 80$).
r	Fan branch regime: ℓ=low-energy regime, H=high-energy regime.